Journal of Materials Chemistry A

Accepted Manuscript

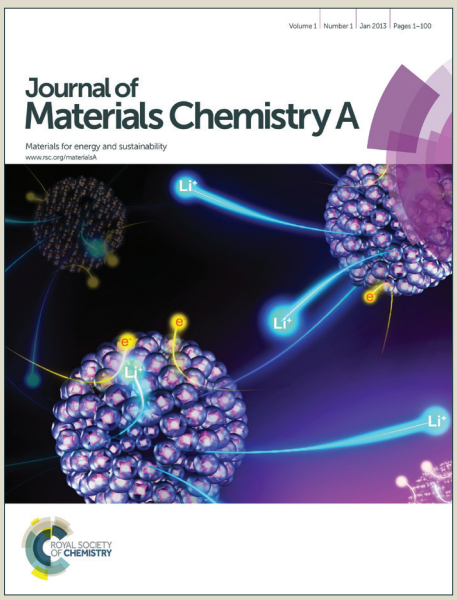

ROYAL SOCIETY OF CHEMISTRY

www.rsc.org/materialsA

Journal of materials chemistry A
Journal of Materials Chemistry A
Dynamic Article Links ►

Cite this: DOI: 10.1039/c0xx00000x

www.rsc.org/xxxxxx

PAPER

A fast route for synthesizing nano-sized ZSM-5 aggregates

Feng Pan[a], Xuchen Lu*[a,c], Qingshan Zhu[a], Zhimin Zhang[a], Yan Yan[a], Tizhuang Wang[a] and Shiwei Chen[a,b]

Received (in XXX, XXX) Xth XXXXXXXXX 20XX, Accepted Xth XXXXXXXXX 20XX
DOI: 10.1039/b000000x

Nano-sized ZSM-5 aggregates have been rapidly synthesized from the leached metakaolin by solid-like state conversion. The influence of synthesis conditions such as TPA^+/SiO_2, $NaOH/SiO_2$ and SiO_2/Al_2O_3 molar ratios on the final products were investigated. The properties of nano-sized ZSM-5 aggregates were characterized by XRD, SEM, HRTEM, ^{29}Si and ^{27}Al MAS NMR, NH_3-TPD, TG, N_2 adsorption/desorption and particle size analysis. The results clearly showed that nano-sized ZSM-5 aggregates could be obtained within 2 h via solid-like state conversion. SEM revealed that the obtained ZSM-5 aggregates were irregular spheres that consisted of nano-sized crystallites with 30-50 nm. Crystallization process indicated that the size of flaky raw materials gradually decreased and formed nano-sized particles as prolonged the time. Therefore, the transformation mechanism abode by solution mediated mechanism, though only a little water was contained in the system. Compared with the conventional hydrothermal route, the solid-like state conversion not only significantly shortened the crystallization time, but also totally avoided the emission of waste liquid. In addition, for the methanol dehydration reaction, the nano-sized ZSM-5 aggregates obtained by this method showed much better catalytic performance, C2-C4 olefins selectivity and longer lifetime to endure coke deposition than the sample obtained by hydrothermal route.

1. Introduction

ZSM-5 is a medium pore zeolite having a 10-membered ring structure with two types of channels, straight and zigzag. It has been widely used as catalysts and selective adsorbents in the petrochemical industry owing to its high thermal stability, intrinsic acidity, high surface area and well-defined porosity[1]. Nano-sized zeolites have a dramatic effect on the rates of diffusion and reaction, which can significantly influence the catalytic performance when it is used as catalysts. Therefore, nano-sized ZSM-5 zeolites have received much attention due to its good performances such as very shape-selective properties, high steam stability, high metal resistance and slow coke accumulation[2, 3]. Various attempts to synthesize ZSM-5 with nano-sized crystals have been developed. In a typical approach, monodispersed or nano-sized aggregates of ZSM-5 was synthesized by carefully controlling the gel composition and crystallizing conditions in the hydrothermal environment[4-6]. However, the crystallization time was as long as several days, the yield of nano-sized ZSM-5 aggregates was no more than 50%. Another strategy is to restrict the growth of the nano crystals, named as confined space[7, 8] or silanization method[9, 10]. Madsen and Jacobsen[8] obtained nano-sized ZSM-5 crystals by using confined space method for the first time. The procedure consisted of incipient wetness impregnation of mesoporous carbon black with a zeolite precursor, then, the carbon black was consequently subjected to autoclave treatment in saturated steam. Serrano et al.[9] adopted organosilane as growth inhibitor to synthesize nano-sized ZSM-5. The synthesis is based on reducing the size of zeolite crystals by silanization of the zeolitic seeds or precusors to hinder their further growth. The obtained sample consisted of 300-400 nm particles which were formed by the aggregation of small units of 10 nm. The third measure is to provide enough crystal nuclei for the formation of nano crystals via adding crystal seeds, called seed-induced crystallization. Majano et al.[11] studied the influence of synthesis parameters on the crystallization of ZSM-5 nanoparticles, established the relationship between the factors and the nanosized zeolite particles, and revealed the formation mechanism of the nanocrystallines.

In fact, the above mentioned methods belong to the traditional hydrothermal route. Some shortcomings are still inevitable, such as time-consuming, low yield, generating a large amount of waste solvents, high cost, and higher requirements for equipment due to the high pressure. If the synthesis are performed in a solvent-free system or directly adopted the solid-state raw material, some obvious advantages could be brought[12, 13]: (1) High yields of products. (2) Reducing the waste liquids significantly. (3) Shortening the crystallization time greatly, and enhancing the production efficiency. (4) Saving energy and simplifying the synthetic procedures. Therefore, solid-state transformation[12], steam-assisted crystallization (SAC), also called vapor-phase-transport or dry gel conversion (DGC) [13-16], have been developed

for the synthesis of zeolites. Especially, the DGC method is also quite effective for the synthesis of nano-sized ZSM-5. It is worth to mention that the DGC or SAC method has gained much attention recently. A series of work have been devoted to synthesize ZSM-5 with nano-sized crystals or hierarchical structure. Zhou et al.[15] obtained highly crystalline ZSM-5 with micro/mesoporous structure by treated for 12 h. More recently, Song[17] and Nandan[18] synthesized hierarchical ZSM-5 consisted of nano crystals via steam-assisted crystallization. The dry-gel conversion method could shorten the crystallization time obviously, enhance the yield of the products, and avoid the emission of waste liquids. Nevertheless, he procedures of dry gel preparation are complicated, in which the solvents are necessary for preparation of the homogeneous gels, followed by vaporizing the solvents to obtain the dry gels[13]. In addition, the organic template could get into the solvent at the bottom of the Teflon. Even so, these abovementioned methods have provided good ideas for the synthesis of nano-sized ZSM-5 or other zeolites.

Actually, ZSM-5 zeolites have been synthesized from chemical silica and aluminium sources in solvent-free system. However, the crystal of the sample was micro-sized particle and crystallization time was as long as 24 h[14]. Compared with the traditional chemical silicon and aluminum sources, natural clay is considered to be an alternative material for the synthesis of zeolites because it is readily available and very economical. Therefore, the conversion of natural clay to crystalline zeolite has been gaining much attention in academic and industrial fields. Kaolin [$Al_2Si_2O_5(OH)_4$] is one pf the most important clays, which is connected by one siliconoxygen (SiO_4) tetrahedral layer and one alumina [$Al(O, OH)_6$] layer. It has been proved a good combinational silicon and aluminum source to synthesize zeolites or functional materials, such as A[19], X[20], mesoporous γ-Al_2O_3[21], SAPOs[22, 23], ZSM-5[24-26], etc.. To obtain nano-sized zeolites, the key point is to control the concentration and supersaturation of crystal nucleus. Kaolin gradually could dissolve into system and formed the crystal nucleus heterogeneously during the crystallization process[21, 22]. Therefore, it is difficult for laminated clays to synthesize ZSM-5 with nano-sized crystal via traditional hydrothermal method.

Based on the ideas of the DGC or SAC method, we tried to further reduce the crystallization time and the emission of the waste solvents. Thus, this paper described the nano-sized ZSM-5 aggregates were fast and directly synthesized by solid-like state transformation using tetrapropylammonium hydroxide (TPAOH) as a template and kaolin as a silica–alumina source. In addition, the catalytic performance of the obtained ZSM-5 by solid-like conversion and traditional hydrothermal route has been compared.

2. Experimental

2.1 Synthesis of nano-sized ZSM-5 aggregates

The raw material powders of kaolin (Inner Mongolia, China) were converted to metakaolin by calcining kaolinite at 1073 K for 2 h. Then, the metakaolin powders were leached with 6 M HCl solution (solid/liquid ratio 1:5, g/ml) with stirring. After that, the leached metakaolin was filtered, washed with deionized water, dried and collected as precursors for the synthesis of nano-sized ZSM-5 aggregates.

In a typical synthesis of nano HZSM-5 zeolite, dealuminated metakaolin was uniformly mixed with NaOH, TPAOH in the molar ratios SiO_2: xAl_2O_3: yTPAOH: zNaOH: mH_2O (the water only came from TPAOH solution) = 1: 25.68-80: 0.026-0.065: 0.012-0.258: 0.89-2.67, and transferred into a 50 ml Teflon-lined autoclave. Then, Teflon-lined autoclave was left stand for 0-3 h at 190 °C. The obtained sample was calcined at 550 °C for 6 h to remove the organic templates. In order to investigate the catalytic performance, the as-synthesized Na-ZSM-5 sample need to transform into H-form ZSM-5, the as-synthesized sample (SiO_2/Al_2O_3 = 37.74) was exchanged with 1 M NH_4NO_3 solution at 90 °C for 2 h, calcined at 550 °C for 6 h, and named as HSZ-5. A contrast sample was synthesized by traditional hydrothermal method[27], and named as HCZ-5.

2.2 Characterization

Powder XRD patterns of the dried solid products were recorded by a PANalytical X'pert diffractometer with CuKa radiation. The morphology and chemical composition of the samples were characterized by field-emission scanning electron microscopy (SEM) (JEM-7001F, JEOL, Japan). Transmission electron microscopy (TEM) images were obtained on a JEM 2100F electron microscope operating at an accelerating voltage of 200 kV. FT-IR spectra were recorded on an ALPHA FT-IR spectrometer (Bruker, Germany) using dried KBr disk technique, in the range of 400-4000 cm^{-1}. N_2 adsorption-desorption were measured on AUTOSORB–1 analyzer (Quantachrome). Prior to measurement, the samples were degassed at 573 K for 10 h under vacuum. Total acidity and acid strength distribution of the catalyst were determined by calorimetric measurement of differential adsorption of NH_3 at 60 °C and subsequent TPD of the adsorbed NH_3 with a ramp of 10 °C min^{-1} up to 700 °C (Quantachrome CHEMBET 3000, USA). Coke amount was determined using a TG/DTA6300 (Japan) thermogravimetric analyzer from 30 to 800°C under air flow with a heating rate of 10°C/min. Particle size analysis were performed on a laser particle size analyzer (Mastersizer 2000E, Malvern). ^{29}Si and ^{27}Al magic angle spinning nuclear magnetic resonance (MAS-NMR) spectroscopy was performed at room temperature using a Bruker Advance III 400 spectrometer operated at 104.0 MHz for ^{27}Al and 79.3 MHz for ^{29}Si. The recycle delay was 1.0 s for ^{27}Al and 2.0 s for ^{29}Si. The pulse duration (or pulse width) was 1.0 μs for ^{27}Al and the contact time was 5.0 ms for ^{29}Si.

2.3 Catalytic performance

Catalytic reaction tests were conducted at 425 °C under atmospheric pressure in a conventional continuous down flow, fixed-bed stainless steel reactor (inner diameter 6 mm). 0.3 g of HZSM-5 catalyst (40-60 mesh) was placed in the center zone of the reactor. Prior to the catalytic measurements, the fresh catalyst was activated at 500 °C for 2 h with nitrogen (15 mL min^{-1}). Then, reactant (50 vol% methanol solution) was pumped into pre-heater reactor through a piston pump (WHSV of ethanol was 7.0 h^{-1}), and got into reactor with nitrogen (15 mL min^{-1}).

The feed and products were analyzed on-line by gas chromatography (SHIMADZU GC-2014) equipped with flame ionization detector (FID) and thermal conductivity detector (TCD). FID with a TG-BOND capillary column (50 m × 0.32 mm × 15 μm, Thermo, USA) analyzed un-reacted methanol, dimethyl ether and hydrocarbons (C1-C5). TCD with a GDX-101 packed column detected CO, H_2 and CO_2. All products were identified according to the standard gases (Beijing Gaisi Chemical Gases Center), and the concentration of the components in the reactor effluent stream, expressed as molar percentages, was determined from the on-line chromatographic results. The response factors in gas chromatography analysis were evaluated from the effective carbon number. In addition, the conversion of methanol to coke was neglected because the instantaneous formation of coke was dependent on reaction time and difficult to estimate. The conversion of methanol was calculated by applying the molar balance between the inlet and outlet of the reactor. Selectivity for the products of interest were expressed as mass percentage of each product and calculated according to the carbon balance between the inlet and the outlet of the reactor.

3. Results and discussion

3.1 Factors affecting the synthesis of nano-sized ZSM-5 aggregates

The presence of TPAOH can promote the condensation reaction between –Si–O–H groups to form –Si–O–Si– groups. In the synthesis of nano-sized zeolites, the high supersaturation conditions are a key factor for the formation of nano-crystalline zeolite. This condition is usually achieved by the utilization proper amounts of organic structure directing agents (SDA). Therefore, the influence of TPAOH content on the structure and morphology of the final products was investigated.

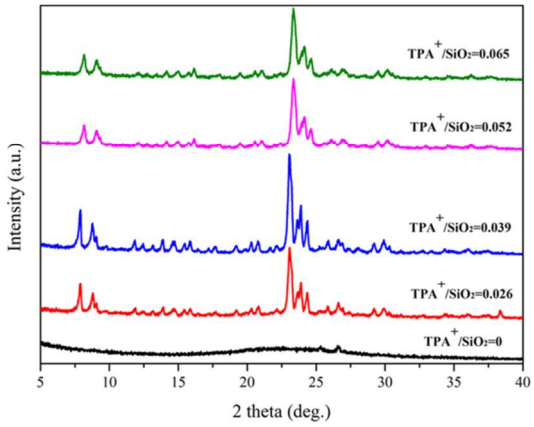

Fig. 1 XRD patterns of as-synthesized samples with different TPA^+/SiO_2 molar ratio

The organic template, TPAOH had four roles in this synthesis system. It served as structure-directing agent in the assembly of the zeolite framework, participated the balance of the framework charge, maintained the alkalinity of the synthesis solution. More importantly, it could provide the solvent for the system. The system with the molar composition of xTPAOH: SiO_2: yH_2O has been studied, where x was between 0.026 and 0.065, y was between 0.89 and 2.67 which depended on the content of TPAOH solution. Fig. 1 shows the XRD patterns of as-synthesized samples with different TPA^+/SiO_2 molar ratio. According to the results, the characteristic diffraction peaks of ZSM-5 appeared when the molar ratio of TPA^+/SiO_2 was as low as 0.026, indicating the leached metakaolin transformed to highly crystalline ZSM-5 within 2 h. This amount of TPAOH was much lower than that of reported by Ren[12]. However, nano-sized ZSM-5 aggregates could not be obtained under this condition, as could be seen in Fig. 2 (a). The intensity of the diffraction peaks decreased, and the half-peak width increased significantly as the amount of TPAOH increased, suggesting that the existence of nano-sized crystalline in the samples[9, 28]. The final particle size decreased from 1 um to 40 nm when the x value of TPAOH increased from 0.026 to 0.052. The results demonstrated that there was a remarkable dependence of the final particle size on the content of TPAOH. Further increasing the TPAOH content (x > 0.052) did not lead to smaller crystals, which was consist with the result reported in the literature[29]. But, the amount of TPAOH used in this system was much lower than that in the reference ($TPA^+/SiO_2 \geq 0.4$)

It could be hypothesized that each TPA^+ cation was an effective site for the formation of pentasil unit. Therefore, higher amount of TPAOH could provide more sites for the formation of initial nuclei of ZSM-5 zeolite, which caused the particle size of ZSM-5 dramatically reduced. Thus, the content of structure directing agent played a very important role in the formation of nano-sized ZSM-5. However, the effect of the little water that contained in the TPAOH solution could not be ignored. ZSM-5 could not be obtained as adopted dried TPABr as structure-directing agent. Therefore, the very small amount of water provided an environment for the dissolution of silicon and aluminium species.

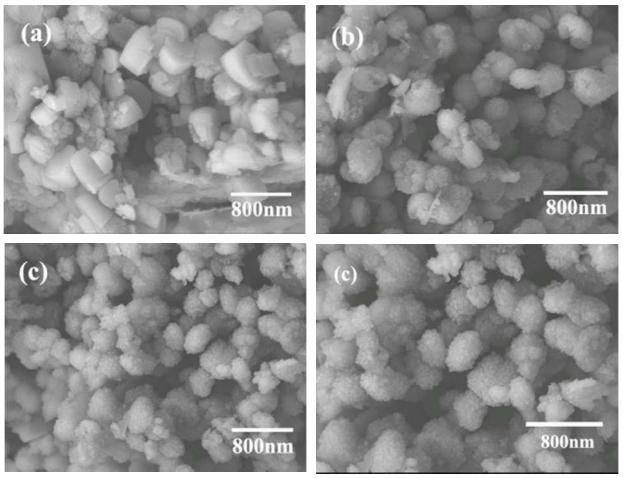

Fig.2 SEM images of as-synthesized samples: (a) TPA^+/SiO_2=0.026; (b) TPA^+/SiO_2=0.039; (c) TPA^+/SiO_2=0.052; (d) TPA^+/SiO_2=0.065

Nano-sized ZSM-5 aggregates could be obtained in such a short time due to the little content of water. The nuclei formed by silicon and aluminum species easily reached supersaturation in the solid-like system, which were a key factor for the formation of nanocrystalline zeolite quickly. Compared with the literature[30],

where 55 nm silicalite-1 particles were synthesized with a molar composition of 3TPAOH: 25SiO_2: 390H_2O at low temperature (<308 K) with a very long synthesis time (40 months), the crystallization time reduced significantly in this system.

The leached metakaolin still contained some metallic elements (such as Fe, Ti, Mg etc.), which might show different crystallization characteristics from the chemical ones. Therefore, it is necessary to investigate the effect of SiO_2/Al_2O_3 molar ratios on the final products. Fig. 3 shows the XRD patterns of the sample with different SiO_2/Al_2O_3 molar ratios. It was evident that all the samples showed strong diffraction peaks except the SiO_2/Al_2O_3 of the sample was 25.68. The results indicated that the precursor with lower SiO_2/Al_2O_3 was not beneficial for the formation of nano-sized ZSM-5 aggregates. As illustrated in Fig. 4a, some flaky material was still visible. This situation might be ascribed to the high content of aluminate ions hindered the increase of the concentration of silicate ions that involved the formation of crystal nuclei[31].

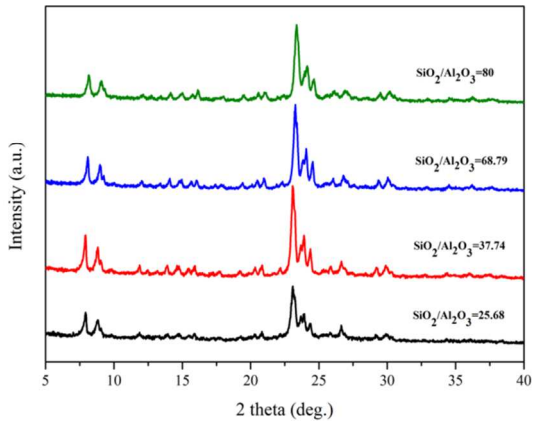

Fig.3 XRD patterns of the samples obtained from leached metakaolin with different SiO_2/Al_2O_3 molar ratio

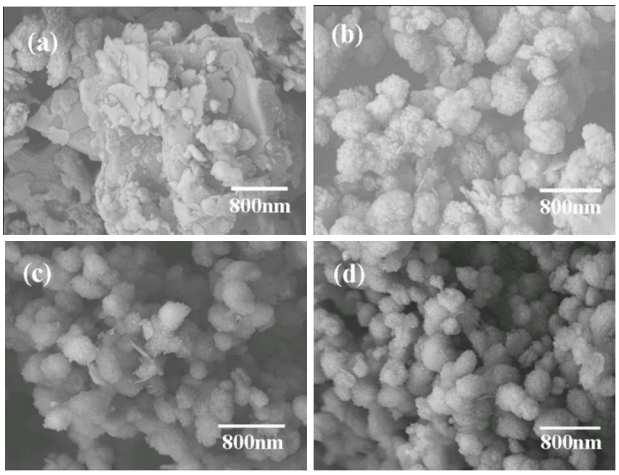

Fig.4 SEM images of the samples obtained from leached metakalin with different SiO_2/Al_2O_3 molar ratio (a) SiO_2/Al_2O_3=25.68; (b) SiO_2/Al_2O_3=37.74; (c) SiO_2/Al_2O_3=68.79; (d) SiO_2/Al_2O_3=80

As the SiO_2/Al_2O_3 increased to 37.74, the intense diffraction peaks of ZSM-5 (JCPDS Card No. 00-044-0002) indicated that highly crystalline nano-sized ZSM-5 could be obtained. From the SEM images (Fig.4 b), the sample presented irregular spherical agglomerates with size of 200-600 nm. The aggregates were composed of nano-sized crystals with ca. 40 nm. Highly crystalline ZSM-5 was still obtained as continuing to increase the silica alumina ratio, and all the three samples had the similar morphology. The results indicated that there was no significant effect on the morphology as the SiO_2/Al_2O_3 molar ratio changed.

Supersaturation of the nuclei can be achieved by the dissolution of excess silicon and aluminum species contained in the precursors. So, the alkalinity of the system should satisfy the requirement of nucleation and crystal growth. As a mineralizer, the hydroxy group of NaOH facilitates the conversion of oxide forms of silicon and aluminum to useful kinds of precursors in tetrahedral coordination and condensation. The crystallization system reaches the state of supersaturation, which is a necessary condition to facilitate the process of nucleation and crystal growth.

According to Fig. 5 (a), the final sample was amorphous phase without adding NaOH, indicating the precursor did not participate in the formation of crystal nuclei and the growth of crystals. The obtained sample was still amorphous though increasing the TPAOH/SiO_2 to 0.065, and prolonging the crystallization time to 24h at 190□. The results demonstrated that NaOH not only provided OH^- to fascinate the polycondensation reaction between silicon and aluminum species, but also supplied Na^+ to balance the charge of framework. The characteristic peaks of ZSM-5 could be detected at 2θ = 22-25° as only few NaOH was added into the reaction system. However, a large amount of precursor did not transform into ZSM-5 because the alkalinity was too weak to make silica and alumina dissolve into the system. The alkalinity increased with the increase of NaOH content, which was beneficial to improve the nucleation rate and shorten the crystallization time. Therefore, as the NaOH/SiO_2 increased to 0.026, the relative crystallinity dramatically increased in such a short time. As could be seem in Fig. 5 (b) and (c), all samples were aggregates that were composed of nano crystals with 40 nm, indicating there was no significant influence on the morphology of final products.

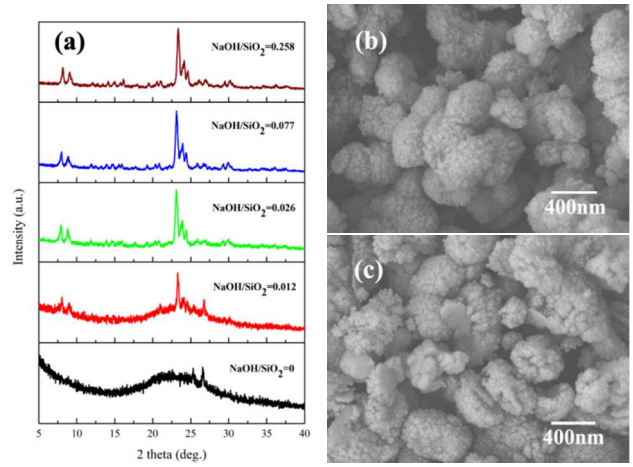

Fig. 5 (a) XRD patterns of the samples obtained at different NaOH content,; SEM images of the sample obtained as (b) NaOH/SiO_2=0.026, (c) NaOH/SiO_2=0.258

3.2 Crystallization process of nano-sized ZSM-5 aggregates

In order to understand the growth process of the nano-sized ZSM-5 aggregates, the products from different crystallization times were studied.

From the XRD patterns (Fig.6 a), the peaks at about 2θ =7-9°, 22-25° began to appear after heating the sample for 0.5 h, the relative crystallinity was only 12%. According to the N_2 adsorption-desorption results (table 1), the specific surface area was only 200.5 $m^2 \cdot g^{-1}$. The relative crystallinity rapidly increased to ca. 90% after treated for 1h. As extended the time to 3 h, no significant change was observed, indicating almost pure ZSM-5 crystals were formed. The S_{BET} of the sample increased to 440.8 $cm^2 \cdot g^{-1}$, which was similar with the value reported in literature[32]. In the IR spectra, the peaks at 550 cm^{-1} and 1221 cm^{-1} which belong to the five-membered ring and the asymmetric stretching vibration of T-O bonds[33] gradually got strong as the time extended[34].

Table 1 the porous properties of synthesized ZSM-5 under different times

Property	0.5h	1.0h	2.0h	3.0h
Total surface area / $(m^2 \cdot g^{-1})^a$	200.5	434.7	446.4	440.8
Micropore area/$(m^2 \cdot g^{-1})^b$	36.8	307.3	305.8	304.7
External surface area/$(m^2 \cdot g^{-1})^b$	163.7	127.4	140.6	136.1
Pore volume / $(cm^3 \cdot g^{-1})^c$	0.27	0.28	0.30	0.27
Micropore volume / $(cm^3 \cdot g^{-1})^b$	0.06	0.12	0.12	0.13
Micropore pore diameter / nm^d	0	0.55	0.55	0.55

a - Determined by BET method from P/P_0 = 0.02-0.07

b - Determined by t-plot method from P/P_0 = 0.4-0.6

c- Caculated at P/P_0 =0.99

d- Determined by HK method

Fig. 6(c) and (d) shows the change of coordination of Al and Si species with the change of the crystallization time. For the initial sample, two resonance peaks at 50 ppm and 0 ppm could be observed in ^{27}Al NMR spectra, which assigned to the tetrahedrally coordinated aluminium in framework and the octahedral non-framework aluminium, respectively[35]. A major peak at −100 ppm with a shoulder centered at −110 ppm could be seen in ^{29}Si NMR spectra, corresponding to Si atoms in Si (1Al) and Si (0Al) configurations[36, 37]. The resonance peak of ^{27}Al NMR at around 0 ppm gradually disappeared as the extension of thermal treatment, which demonstrated that the octahedral non-framework aluminium transformed into the tetra-coordinated Al. The coordination of Si species changed dramatically during the crystallization process. The peak at -100 ppm disappeared, while the peak at -110ppm was gradually enhanced, the results indicated that the coordination of Si species changed from Si (1Al) (Q_3) to Si (0Al) (Q_4). Furthermore, the peaks assigned to Q_3 and Q_4 shifted from -100 ppm to -102 ppm, -110 ppm to -115 ppm, respectively. This phenomenon might be ascribed to the bond angle of Si-O-Si in ZSM-5 was bigger than the one in amorphous silica[38]. The remarkable decrease in the Q^3/Q^4 ratio indicated the hydrophilic surface transformed into a hydrophobic one, or in other words, the amorphous aluminosilicate wall was converted into crystallized zeolite frameworks.

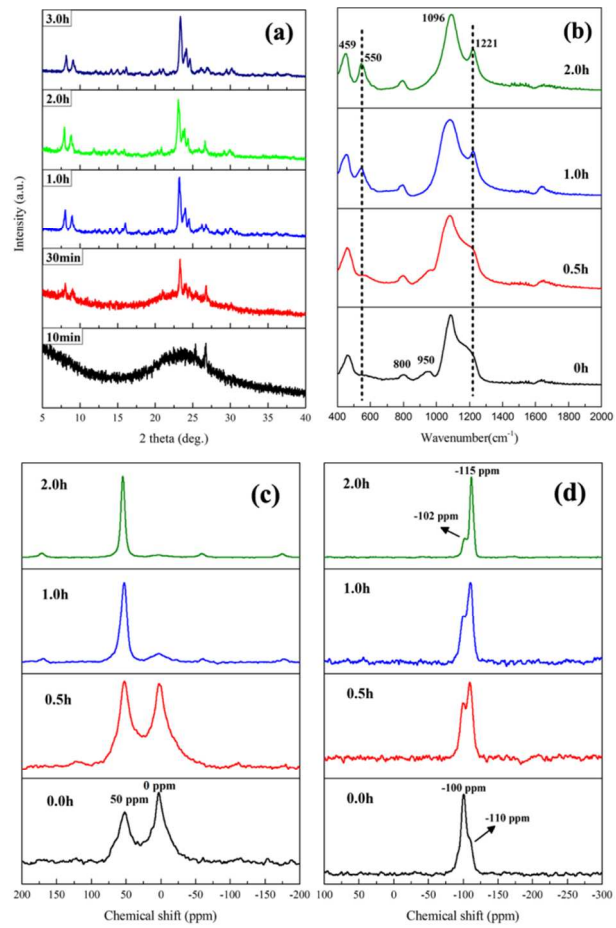

Fig. 6 (a) XRD patterns, (b) IR spectra, (c) ^{27}Al NMR and (d) ^{29}Si NMR of the samples obtained at different crystallization time

3.3 Scheme for the formation of nano-sized ZSM-5 aggregates

Typical clay minerals like kaolin have received special attention because of their potential use in intercalation nanocomposites in which their unique layered structure can play a key role [39]. So, it is necessary to discuss the interaction between leached metakaolin and other materials.

Firstly, due to its special layered and porous structure, the leached metakalin might combined with TPA^+ via chemical bonds (-OH) or acting force (eg. Van der Wals forces). In order to clarify the interaction between the leached kaolin and TPA^+, the leached kaolin (K) and leached kaolin treated with TPAOH at room temperature (TK) were detected on TG and N_2 adsorption/desorption apparatus (Fig. 7). For the TK sample, there was an obviously mass loss peak in the second stage, which was attributed to the decomposition of TPAOH[13]. The result proved that the TPAOH was still kept in the leached kaolin after washed with water. Furthermore, the total surface area decreased obviously from 481.8 $m^2 \cdot g^{-1}$ to 250.4 $m^2 \cdot g^{-1}$, and the total pore volume decreased from 0.38 $cm^3 \cdot g^{-1}$ to 0.25 $cm^3 \cdot g^{-1}$, after treated with TPAOH (table 2). the results indicated that TPA^+ cations have been inserted into the leached kaolin[12]. The above results implied that the TPAOH molecules adsorbed onto the outer

surfaces of kaolin or between the layers of leached kaolin was not a simple physical adsorption.

Table 2 the porous properties of as-synthesized HKZ-5 and HCZ-5

Property	Leached Kaolin treated with TPAOH	Leached Kaolin
Total surface area / $(m^2 \cdot g^{-1})^a$	250.4	481.8
Micropore area/$(m^2 \cdot g^{-1})^b$	77.6	233.4
External surface area/$(m^2 \cdot g^{-1})^b$	172.8	248.4
Pore volume / $(cm^3 \cdot g^{-1})^c$	0.25	0.38
Micropore volume / $(cm^3 \cdot g^{-1})^b$	0.037	0.10

a - Determined by BET method from P/P0 = 0.02-0.07

b - Determined by t-plot method from P/P0 = 0.4-0.6

c- Caculated at P/P0 =0.99

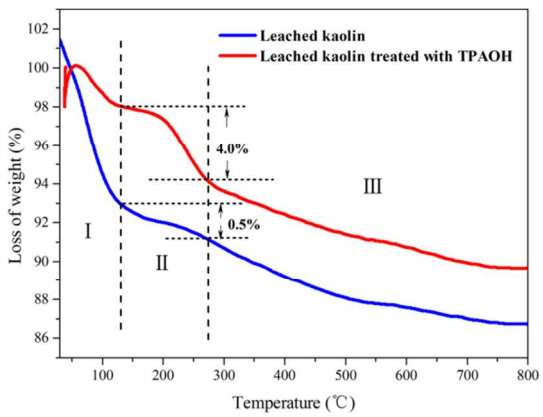

Note: the leached kaolin treated with TPAOH was obtained by following procedures: the leached kaolin was mixed with TPAOH (25% solution) uniformly, and let stand for 2 h at room temperature. Then, the mixture was washed with water, filtered and dried.

Fig. 7 TG curves of leached kaolin and leached kaolin treated with TPAOH

Secondly, the leached metakaolin dissolved gradually into the system under the alkaline condition. To prove this phenomenon, the products obtained from different crystallization times were characterized by SEM and TEM (Fig. 8). The size of flaky raw materials gradually decreased, the edge of the materials became smooth, as prolonged the crystallization time. In addition, some small holes emerged on the surface of the precursor, as could be seen the inserted image in Fig. 8 (A)-(b). This phenomenon indicated that metakaolin dissolved and formed silicate and aluminate ions that formed the elementary units of ZSM-5.

Thirdly, the silicate ions and aluminate ions were formed by the dissolution of leached kaolin under alkaline condition. Generally, the final crystal size distribution strongly depends on the total number of nuclei formed during the crystallization and on the rate of their formation[40, 41]. It is worth to mentioning that ZSM-5 cannot be obtained in the absence of NaOH by solid-like state conversion. So, it could be deduced that the addition of NaOH provided alkalinity to dissolve the solid materials and Na^+ to balance the charge of the skeleton. In addition, as previously described, no ZSM-5 phase could be generated in the final products as the system definitely did not contain water. Therefore, the little water contained in the TPAOH was critical for the formation of zeolites in the solid-like state system. According to Chang[42], the silicon species contacted with TPA^+ by van der Waals interaction, and formed embryonic structures rapidly upon heating by formation of chlatrate-like water structure around TPA^+, following by a fast isomorphous substitution of silicate for water. So, it was beneficial for the nuclei to get supersaturation in the solid-like state system.

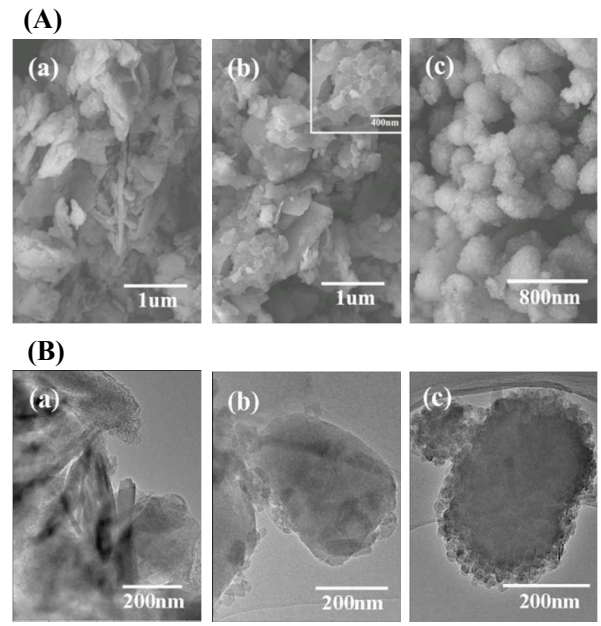

Fig. 8 SEM (A) and TEM (B) images of the samples obtained at different times: (a) 0h, (b) 0.5h, (c) 2h.

Finally, the nuclei grew into nano-sized ZSM-5 aggregates. After the nuclei formation, a fast crystal growth of ZSM-5 happened probably by the continuous assembly of the nuclei. Thereafter, the solid surface was further dissolved, gelated, and a continuous migration took place from the solid surface to the colloid until it was depleted. The crystal nuclei gradually grew into nano-sized ZSM-5, and aggregated together due to the high activity of the nano crystals, as could be seen in the TEM images (Fig. 8 (B)).

Therefore, the schematic of crystallization mechanism for the nano-sized ZSM-5 aggregates could be illustrated as follows:

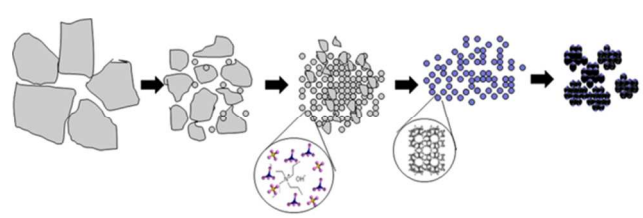

Fig. 9 Schematic of growth mechanism for the nano-sized ZSM-5 aggregates

3.4 Catalytic performance

As illustrated in Fig. 10 (a) and (b), the morphology of ZSM-5 synthesized by solid-like state conversion and hydrothermal route exhibited significance difference. The d_{50} particles of both samples were 427 nm and 6.4 μm, which was good agreement with the SEM results. HSZ-5 catalysts showed very high activity to convert methanol completely to hydrocarbons in the initial 20 hours (Fig. 10 (d)). After that, the activity of HSZ-5 declined slightly and the conversion of methanol was sustainably higher than 95% after 27 h. In sharp contrast, conversion of methanol over HCZ-5 dropped to 78% after 27 h. Generally, the deactivation of zeolite catalysts occurs predominantly by the poisoning of acid sites and/or the pore blocking due to the accumulation of carbonaceous deposits. The products easily diffused out of the pores in HSZ-5 because of the existence of nano-sized crystal, which retarded the secondary reaction to form the precursor of coke and hence delay the blocking of the channel by coke[43]. Therefore, the ability of resistance carbon deposition on HSZ-5 was better than that on HCZ-5 zeolite, this conclusion could be proved by the TG results (Fig. 10 f).

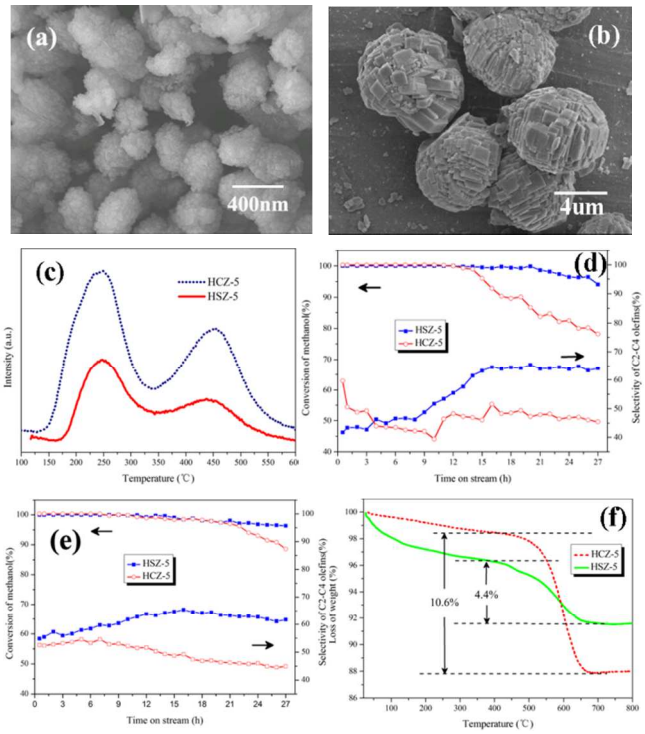

Fig. 10 (a) SEM image of ZSM-5 obtained by solid-like state conversion; (b) SEM image of ZSM-5 obtained by hydrothermal route; (c) NH_3-TPD curves of HSZ-5 and HCZ-5; (d) Methanol conversions and C2-C4 olefins selectivity on the fresh zeolites as a function of time-on-stream; (e) Methanol conversions and C2-C4 olefins selectivity on the regenerated zeolites as a function of time-on-stream; (f) TG curves of HSZ-5 and HCZ-5 after MTO reaction.

As the reaction time prolonged, selectivity of C2-C4 olefins on HCZ-5 catalyst gradually decreased to ca. 40%, then increased to ca. 46%. In a sharp contrast, though the conversion of methanol decreased to 95%, the HSZ-5 catalyst was still favorable to the formation of C2-C4 olefins. The selectivity of olefins over HSZ-5 continued to increase to ca. 65%. Due to the smaller crystal size of HSZ-5, the coke formation rate over HSZ-5 was slower than that over HCZ-5. Moreover, appropriately coke deposit can reduce the size of channel, which was beneficial to enhance the selectivity of C2-C4 olefins. In addition, the lower surface acidity of HSZ-5 contributed to the higher selectivity of C2-C4 olefins, as described by Inoue et al.[44], lower surface acidity played vital roles in the formation of olefins in methanol dehydration reaction, while aromatics were promoted at higher acidity. Though the MTO reaction was closely related to the strong acid sites, the amount of strong acidity should be appropriate. As showed in Table 3, the HSZ-5 catalyst had the lower concentration of strong acid sites than that of HCZ-5. Therefore, it was beneficial for the formation of light olefins.

Table 3 the porous properties of as-synthesized HSZ-5 and HCZ-5

Property	HSZ-5	HCZ-5
Total surface area / $(m^2 \cdot g^{-1})^a$	446.4	354.3
Micropore area/$(m^2 \cdot g^{-1})^b$	305.8	311.9
External surface area/$(m^2 \cdot g^{-1})^b$	140.6	42.4
Pore volume / $(cm^3 \cdot g^{-1})^c$	0.30	0.23
Micropore volume / $(cm^3 \cdot g^{-1})^b$	0.13	0.13
Weak acidity / (NH_3, mmol/g)^d	0.33	0.62
Strong acidity / (NH_3, mmol/g)^d	0.12	0.45

a - Determined by BET method from P/P0 = 0.02-0.07

b - Determined by t-plot method from P/P0 = 0.4-0.6

c- Caculated at P/P_0 =0.99

d- weak acidity: from 373 to 643 K; strong acidity: from 643 to 823 K. both the weak and strong acidity were quantified by titration.

To investigate the regeneration ability of the nano-sized ZSM-5 aggregates, the reacted HSZ-5 was burned off under a flow of dried air (15 mL min^{-1}) at 823K for 2 h. Then, the regenerated HSZ-5 and HCZ-5 were used for the recycle reaction. As showed in Fig. 10 (e), after 27 hours of continuous running, methanol could still maintain a higher conversion rate on regenerated HSZ-5. Compared with the fresh HSZ-5, the selectivity of C2-C4 olefins was much higher in the initial stage. It was interesting that the conversion of methanol on HCZ-5 much better than the fresh one, and the C2-C4 olefins increased obviously in the initial stage. This phenomenon might be ascribed to the dealumination of the catalyst that happened during the reaction due to the presence of water. In addition, the selectivity of the olefins on regenerated HSZ-5 had the similar tendency with the fresh one, and showed much better catalytic performance than the regenerated HCZ-5. The results indicated that the HSZ-5 had excellent regeneration ability.

4. Conclusions

In conclusion, a facile and fast approach has been developed for the synthesis of nanocrystals aggeregates via solid-like state conversion. The obtained ZSM-5 aggregates were irregular spheres with crystal size of 200-500 nm, which consisted of nano-sized crystallites with 30-50 nm. The obtained sample showed good catalytic performance and regeneration ability in the MTO reaction. This method provided an easy and effective path for the synthesis of nano zeolites. In addition, natural layered clays like kaolin, sepiolite and montmorillonite can be used as the

raw materials for the synthesis of many other zeolites, such as ZSM-5, zeolite A, zeolite X, zeolite Y. Therefore, this synthesis approach may be a general way to produce different monodispersed or nano-sized aggregates zeolites.

Acknowledgements

The authors would like to thank Wuhai Tian-yu Chemical High-tech Co. Ltd. (China) for the financial and raw materials assistance

Notes and references

[a] *State Key Laboratory of Multiphase Complex Systems, Institute of Process Engineering, Chinese Academy of Sciences, No. 1 Bei-er-tiao, Zhong-guan-cun, Haidian District. Beijing 100190, P. R. China. Tel: +86 10 8254 4889; E-mail: xclu@home.ipe.ac.cn*
[b]*University of Chinese Academy of Sciences, Beijing 100039, PR China*
[c]United Research Center for Resource and Materials, Wuhai 016000, PR China

1. C. S. Cundy and P. A. Cox, *Chem. Rev.* , 2003, **103**, 663-702.
2. Y. Adewuyi, D. Klocke and J. Buchanan, *Appl. Catal., A*, 1995, **131**, 121-133.
3. L. Tosheva and V. P. Valtchev, *Chem. Mater.* , 2005, **17**, 2494-2513.
4. W. Song, R. Justice, C. Jones, V. Grassian and S. Larsen, *Langmuir*, 2004, **20**, 8301-8306.
5. R. Van Grieken, J. Sotelo, J. Menendez and J. Melero, *Microporous Mesoporous Mater.* , 2000, **39**, 135-147.
6. T. M. Davis, T. O. Drews, H. Ramanan, C. He, J. Dong, H. Schnablegger, M. A. Katsoulakis, E. Kokkoli, A. V. McCormick and R. L. Penn, *Nat. Mater.* , 2006, **5**, 400-408.
7. C. H. Jacobsen, *Chem. Commun.* , 1999, 673-674.
8. I. Schmidt, C. Madsen and C. J. Jacobsen, *Inorg. Chem.* , 2000, **39**, 2279-2283.
9. D. P. Serrano, J. Aguado, J. M. Escola, J. M. Rodríguez and Á. Peral, *Chem. Mater.* , 2006, **18**, 2462-2464.
10. Y.-P. Guo, H.J. Wang, Y.J. Guo, L.H. Guo, L.F. Chu and C.X. Guo, *Chem. Eng. J.* , 2011, **166**, 391-400.
11. G. Majano, A. Darwiche, S. Mintova and V. Valtchev, *Ind. Eng. Chem. Res.* , 2009, **48**, 7084-7091.
12. L. Ren, Q. Wu, C. Yang, L. Zhu, C. Li, P. Zhang, H. Zhang, X. Meng and F.S. Xiao, *J. Am. Chem. Soc.* , 2012, **134**, 15173-15176.
13. R. Cai, Y. Liu, S. Gu and Y. Yan, *J. Am. Chem. Soc.* , 2010, **132**, 12776-12777.
14. P. H. PrasadáRao, *Chem. Commun.* , 1996, 1441-1442.
15. J. Zhou, Z. Hua, J. Zhao, Z. Gao, S. Zeng and J. Shi, *J. Mater. Chem.* , 2010, **20**, 6764-6771.
16. K. Shen, N. Wang, W. Qian, Y. Cui and F. Wei, *Catalysis Science & Technology*, 2014, **4**, 3840-3844.
17. Y. Song, Z. Hua, Y. Zhu, J. Zhou, X. Zhou, Z. Liu and J. Shi, *J. Mater. Chem.* , 2012, **22**, 3327-3329.
18. D. Nandan, S. K. Saxena and N. Viswanadham, *J. Mater. Chem. A*, 2014, **2**, 1054-1059.
19. M. Alkan, Ç. Hopa, Z. Yilmaz and H. Güler, *Microporous Mesoporous Mater.* , 2005, **86**, 176-184.
20. I. Caballero, F. G. Colina and J. Costa, *Ind. Eng. Chem. Res.* , 2007, **46**, 1029-1038.
21. F. Pan, X. Lu, T. Wang, Y. Wang, Z. Zhang, Y. Yan and S. Yang, *Mater. Lett.* , 2012.
22. T. Wang, X. Lu and Y. Yan, *Microporous Mesoporous Mater.* , 2012.
23. J. Zhu, Y. Cui, Y. Wang and F. Wei, *Chem. Commun.* , 2009, 3282-3284.
24. S. M. Holmes, S. H. Khoo and A. S. Kovo, *Green Chem.* , 2011, **13**, 1152-1154.
25. K. Shen, W. Qian, N. Wang, J. Zhang and F. Wei, *J. Mater. Chem. A*, 2013, **1**, 3272-3275.
26. F. Pan, X. Lu, Y. Wang, S. Chen, T. Wang and Y. Yan, *Microporous Mesoporous Mater.* , 2014, **184**, 134-140.
27. C. D. Madhusoodana, R. N. Das, Y. Kameshima and K. Okada, *J. Porous Mater.* , 2005, **12**, 273-280.
28. M. Choi, K. Na, J. Kim, Y. Sakamoto, O. Terasaki and R. Ryoo, *Nature*, 2009, **461**, 246-249.
29. Q. Li, S. Yang and A. Navrotsky, *Microporous Mesoporous Mater.* , 2003, **65**, 137-143.
30. R. W. Corkery and B. W. Ninham, *Zeolites*, 1997, **18**, 379-386.
31. E. G. Derouane, S. Determmerie, Z. Gabelica and N. Blom, *Applied Catalysis*, 1981, **1**, 201-224.
32. D. Serrano, J. Aguado, J. Rodriguez and A. Peral, *J. Mater. Chem.* , 2008, **18**, 4210-4218.
33. G. Lei, B. Adelman, J. Sarkany and W. Sachtler, *Appl. Catal., B*, 1995, **5**, 245-256.
34. J. Jansen, F. Van der Gaag and H. Van Bekkum, *Zeolites*, 1984, **4**, 369-372.
35. W. Guo, C. Xiong, L. Huang and Q. Li, *J. Mater. Chem.* , 2001, **11**, 1886-1890.
36. R. Ryoo and J. M. Kim, *Journal of the Chemical Society, Chemical Communications*, 1995, 711-712.
37. A. Steel, S. W. Carr and M. W. Anderson, *Chem. Mater.* , 1995, **7**, 1829-1832.
38. S. L. Burkett and M. E. Davis, *Chem. Mater.* , 1995, **7**, 920-928.
39. P. Podsiadlo, A. K. Kaushik, E. M. Arruda, A. M. Waas, B. S. Shim, J. Xu, H. Nandivada, B. G. Pumplin, J. Lahann and A. Ramamoorthy, *Science*, 2007, **318**, 80-83.
40. S. Bosnar, T. Antonić-Jelić, J. Bronić, I. Krznarić and B. Subotić, *J. Cryst. Growth* 2004, **267**, 270-282.
41. C. S. Cundy and P. A. Cox, *Microporous Mesoporous Mater.* , 2005, **82**, 1-78.
42. C. D. Chang and A. T. Bell, *Catal. Lett.* , 1991, **8**, 305-316.
43. X. J. Cheng, X. S. Wang and H. Y. Long, *Microporous Mesoporous Mater.* , 2009, **119**, 171-175.
44. K. Inoue, K. Okabe, M. Inaba, I. Takahara and K. Murata, *Reaction Kinetics, Mechanisms and Catalysis*, 2010, **101**, 477-489.

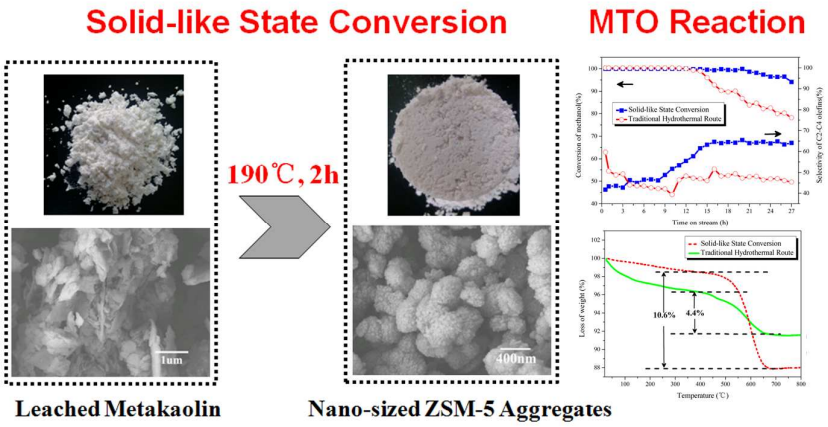

Nano-sized ZSM-5 aggregates have been rapidly synthesized from the leached metakaolin by solid-like state conversion. Compared with the conventional hydrothermal route, the nano-sized ZSM-5 aggregates obtained by this method showed more excellent catalytic performance, C2-C4 olefins selectivity and longer lifetime to endure coke deposition.